RSC Mechanochemistry

ROYAL SOCIETY OF CHEMISTRY

PAPER

View Article Online
View Journal | View Issue

Cite this: *RSC Mechanochem.*, 2024, **1**, 289

The role of the milling environment on the copper-catalysed mechanochemical synthesis of tolbutamide†

Kathleen Floyd, [a] Lori Gonnet, [b] Tomislav Friščić *[b] and James Batteas *[ac]

We provide a systematic investigation of the role of atmospheric oxygen and choice of milling assembly (*i.e.*, the milling jar and ball materials) on a prototypical medicinal mechanochemistry reaction: the copper-catalysed coupling of isocyanate and sulfonamide to form the sulfonylurea tolbutamide. Using in-house developed equipment for work under controlled-atmosphere milling conditions, we reveal that the reaction is in fact catalysed by Cu(II) species, with the conventionally used CuCl acting as a pre-catalyst, which becomes activated *via* aerobic oxidation during milling. Unexpectedly, the choice of milling jar material was found to have a profound effect on the coupling, with aluminium jars effectively "shutting down" reactivity, most likely by preventing CuCl oxidation. Hence, opposite to direct mechanocatalysis, a term used to describe reactions promoted by the milling jar or ball material, this observation reveals the possibility of direct mechanoinhibition – *i.e.*, the inhibition of a mechanochemical reaction by the jar. These results highlight the importance of systematic investigations of both the milling assembly, as well as atmosphere, in understanding and controlling organic mechanochemical transformations.

Received 2nd April 2024
Accepted 6th May 2024

DOI: 10.1039/d4mr00031e

rsc.li/RSCMechanochem

1. Introduction

Mechanochemical reactions, typically conducted by manual grinding, ball-milling, screw extrusion or other types of mechanical impact and shear,[1–4] have emerged as a versatile, general route for conducting solventless synthesis. Mechanochemistry offers excellent atom economy,[5,6] reduced energy consumption,[7,8] and expanded scope of chemical reactivity due to the lack of solubility constraints[9,10] and altered reaction energy landscapes.[11,12] So far, mechanochemical methods have been used towards a wide range of targets, from advanced materials such as metal–organic and covalent-organic frameworks (MOFs, COFs),[13–16] electrides,[17] and pharmaceutical solids, to active pharmaceutical ingredients (APIs).[18–20] Despite growing interest, the mechanisms underlying mechanochemical reactions remain poorly understood, and an area of active investigation. This is particularly true for catalysis under mechanochemical conditions, where research has been mainly on catalyst choice and presence of additives,[21–26] with much less focus on other parameters of the mechanochemical environment, such as the materials of milling assemblies (jars, balls), humidity, atmosphere, *etc*.[27–30] This contrasts the fields of inorganic and coordination mechanosynthesis, where effects of humidity, as well as the participation of milling vessel materials in reactions, are well documented.[31–33] The need to develop an understanding of how the milling assembly could affect catalysis is evident from the recently established phenomenon of direct mechanocatalysis, where the milling balls and/or jar material is found to catalyse reactions either by design or inadvertently.[34–36]

Here we provide a systematic analysis of how the choice of milling assembly and atmosphere affect the well-known copper-catalysed mechanochemical coupling of a sulfonamide with an isocyanate to form the API tolbutamide (see Fig. 1a).[20,37–40] This reaction was chosen as it is an excellent model of API mechanosynthesis. For example, it was recently used for systematic exploration of the effect of the amount of liquid additive (measured as the η-parameter: the ratio of liquid volume to the weight of reacting substances[13–16]) in liquid-assisted reactions by ball milling and resonant acoustic mixing.[41–43] While the mechanochemical milling reaction, whose development was based on an earlier reported synthesis in *N*,*N*-dimethylformamide (DMF) solution by Cervelló and Sastre,[44] was previously found to be catalysed by the addition of either Cu(I) or Cu(II) salts, or even metallic copper, the true catalytic species under mechanochemical conditions has remained unknown.

By systematically controlling the oxygen content in the atmosphere within the milling jars (see Fig. 1b), we

[a]*Department of Chemistry, Texas A&M University, College Station, TX 77842-3012, USA. E-mail: batteas@chem.tamu.edu*

[b]*School of Chemistry, University of Birmingham, Edgbaston, Birmingham B152TT, UK. E-mail: t.friscic@bham.ac.uk*

[c]*Department of Materials Science and Engineering, Texas A&M University, College Station, TX 77842-3012, USA*

† Electronic supplementary information (ESI) available: Chemical details, notes on general procedures and methods, representative product verification data, additional XPS and PXRD data, additional catalyst loading data, and photographs of reaction mixtures. See DOI: https://doi.org/10.1039/d4mr00031e

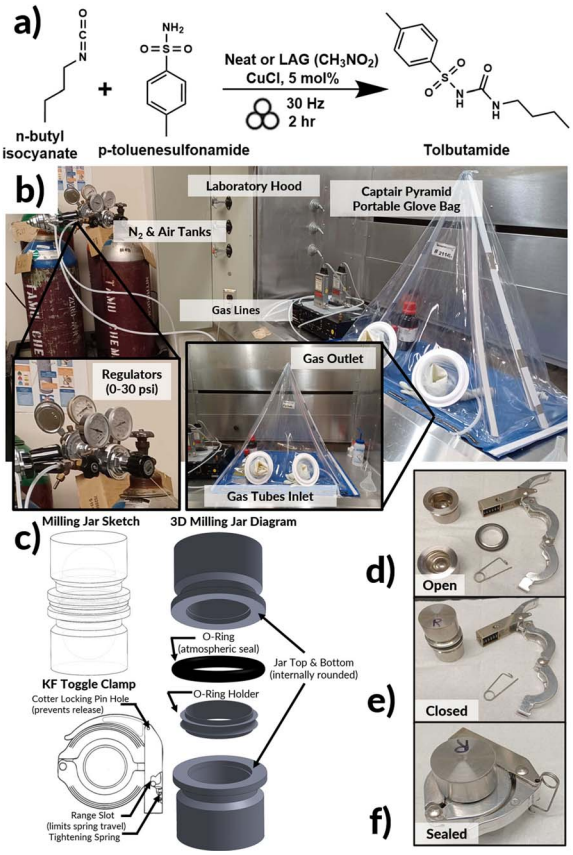

Fig. 1 (a) Scheme for the herein studied mechanochemical catalytic reaction. In-house developed equipment for milling under controlled atmosphere: (b) the laboratory set-up; (c) sketch (left), three-dimensional (3D) diagram (right) for the air-tight milling jars, and associated KF toggle locking clamp mechanism (bottom); (d)–(f) photographs illustrating the assembly and locking of the air-tight milling jars. For examples of equipment developed previously for work under gas flow, or analysing gases coming out of a mill, see ref. 16.

demonstrate that the true catalytic species in this reaction[37,38] appears to be Cu(II). Moreover, the reaction with CuCl as the pre-catalyst exhibits surprising sensitivity to the choice of milling assembly. Whereby the use of in-house manufactured aluminium (Al) -based milling jars lead to the complete "switching off" of the reaction, with the Al metal preventing aerobic oxidative activation of the CuCl. This opposition of the milling process to catalyse the reaction, we refer to as direct mechanoinhibition. This contrasts the established phenomenon of mechanocatalysis where the milling material acts as a reaction catalyst.[34,45–49] Lastly, with Cu(II) being identified as the active catalyst in the reaction, we also explored the effects of catalyst loading on the reaction yield. These studies provide a guide to future systematic investigations of milling environments of other reactions.

2. Materials and methods

Chemicals were purchased from Alfa Aesar, Thermo Scientific, or Sigma Aldrich and used without further purification (see Section 1 of the ESI† for further details).

2.1. Powder X-ray diffraction

Powder X-ray diffraction patterns were collected using a Bruker D8 Endeavor diffractometer at room temperature (using Cu-Kα radiation, with a fixed divergence slit 0.6 mm, sample to anti-air scatter slit distance of 1 mm, LynxEye XE-T detector and PSD opening of 4°) in the two-theta range 5–60° with a step size and time of 0.02° and 1 s respectively. Basic analysis was carried out using the Bruker Diffrac. EVA software.

2.2. X-ray photoelectron spectroscopy

X-ray photoelectron spectroscopy (XPS) data were obtained using a Kratos X-ray Photoelectron Spectrometer – Axis Ultra DLD (detection limit: 0.1 to 1 atomic %) outfitted with a specialized ROX interface (U.S. Patent Application Serial No. 14/445,650 filed July 29, 2014) for transfer of air sensitive samples from a sealed glove box to the surface analysis chamber. Spectra were processed and fit with a Shirley Background and Gaussian–Lorentzian 70 : 30 line-shape using CasaXPS software.

2.3. Nuclear magnetic resonance

^{1}H NMR spectra were obtained with a Bruker Advance Neo 400 instrument equipped with a 400 MHz Ascend magnet, an automated tuning 5 mm broadband iProbe, and a 60 position SampleXpress sample changer. ^{13}C NMR spectra for product verification were obtained on a Bruker Avance III console equipped with a 500 MHz Oxford magnet, an automated tuning 5 mm ^{1}H/^{13}C/^{15}N cold probe, and a 24 position SampleCase sample changer. Reaction tracking in solution was obtained on a Bruker Avance Neo 500 instrument equipped with a 500 MHz Ascend magnet, an automated tuning 5 mm broadband iProbe, and a 16 position SampleXpress Lite sample changer.

2.4. Liquid chromatography mass spectrometry

Electrospray ionization (ESI) was obtained on a Thermo Scientific QE Focus instrument for product verification (see Section 4 of the ESI†).

2.5. Custom milling jars

2.5.1. Milling jars of different materials. Trials employed the following milling materials: 316 stainless steel (SS) milling jars (15 mm diameter SS balls or 12.7 mm diameter polytetrafluoroethylene (PTFE) balls), PTFE milling jars (15 mm diameter SS balls or 12.7 mm PTFE balls), and Multipurpose 6061 Al milling jars (12.7 mm PTFE balls). Milling jars made of different materials were machined in house with 25 mL internal volume. For material suppliers see Section 2.1 of the ESI.†

2.5.2. Milling jars with KF compression seal. In order to enable milling under strictly controlled atmospheres we used in-house designed air-tight milling jars manufactured from 316 SS (see Fig. 1b–f, see also Section 2.2 of the ESI†). The jars are equipped with KF-25 flange vacuum joints which can be sealed with a KF-25 toggle clamp and locking pin (see Fig. 1b–f, see also Section 2.2 of the ESI†).

2.6. Reactions under controlled atmospheres with varying oxygen content‡

2.6.1. General procedure for CuCl experiments. Tolbutamide syntheses with CuCl were performed in a Retsch MM400 mixer mill operating at a frequency of 30 Hz using custom SS KF compression seal jars (see Fig. 1b–f, see also Section 2.2 of the ESI†). Immediately before each experiment, milling jars and balls were cleaned with SS wool using Alconox Detergent cleaning concentrate and water, rinsed under EtOH, and dried under streaming N_2 (g). In a typical experiment, a stainless-steel ball (15 mm diameter, weight ~13.4 grams),§ a mixture of *p*-toluenesulfonamide (214 mg, 1.25 mmol), *n*-butyl isocyanate (140.8 μL, 1.25 mmol), CuCl (6–7 mg, 5 mol%), and in LAG trials only nitromethane (86.0 μL, $\eta = 0.25$ μL mg^{-1}) were placed into custom stainless-steel jars. The jars were purged with 20 psi in a Captair Pyramid Portable Glove Bag with mixtures of nitrogen and dried air (see Fig. 1a). An Omega RH82 hygrometer reading of 0.1% was used to confirm when purging was complete. The content of oxygen (in vol%) was measured using a Forensics NIST calibrated gas monitor (AQ-ODP5-281U). Upon purging, jars were sealed, placed in the Retsch MM400, and the reaction mixtures ball-milled for 2 h.

After the reaction, a small amount of crude product (5–25 mg) was collected from multiple jar regions and dissolved in DMSO-d_6. The isolated product samples were pipetted through a filter pipette to remove CuCl metal contaminant and ^{1}H NMR spectrum of the crude mixture was measured for yield determination. Reaction in DMSO-d_6 did not proceed significantly in an NMR tube when employing pure CuCl as a catalyst. However, reaction in DMSO-d_6 was found to proceed to a limited extent in an NMR tube when employing $CuCl_2$ as a catalyst. To ensure the accuracy of NMR for yield determination, reaction in solution was tracked in an NMR tube using identical amounts of the reagents as employed in the mechanochemical reaction to establish an upper bound for reaction in solution (see Section 3.1 of the ESI†).

2.6.2. General procedure for $CuCl_2$ experiments. The reactions with $CuCl_2$ were run under N_2 or dry air using an identical procedure to that above, but simply substituting the catalyst that was employed ($CuCl_2$, 6–8 mg, 5 mol%). Reaction in DMSO-d_6 was found to proceed to a limited extent in an NMR tube when employing $CuCl_2$ as a catalyst. Again, to ensure the accuracy of NMR for yield determination, reaction in solution was tracked in an NMR tube using identical amounts of the reagents as employed in the mechanochemical reaction to establish an upper bound for reaction in solution (see Section 3.1 of the ESI†).

2.6.3. PXRD analysis. Following a previously described procedure, a total of 7.5 mL of water and $Na_2H_2EDTA \cdot 2H_2O$ (50 mg, 0.17 mol) were added to the remaining crude reaction mixture and milled for 10 min.[37,38] The product was separated by vacuum filtration, rinsed using 80 mL of nanopure H_2O (18.2 MΩ cm, Barnstead) and dried in a Accutemp AT09 vacuum oven at 700 mmHg over P_4O_{10} at 25 °C overnight. Purified product was dissolved in DMSO-d_6. The sample for analysis was passed through a filter pipette and ^{1}H NMR spectrum of the purified product recorded (see Sections 4 and 5 of the ESI†). Based on PXRD analysis, in almost all cases, only polymorph 1 of tolbutamide was observed; see Sections 8 and 9 of the ESI†).[50]

2.7. Reactions under dry air with different milling materials‡

The same procedures used in 2.6 were employed here, except now, the syntheses were run in a series of different milling jars under dried air or N_2 (g) using either CuCl (6–7 mg, 5 mol%) or $CuCl_2$ (6–8 mg, 5 mol%). Briefly, jars were loaded with the reagents, purged under the desired atmosphere, and sealed tightly with parafilm (for the PTFE and the Al jars) or with KF toggle clamps for the SS jars. The milling assemblies used included: (1) SS milling jars (15 mm SS balls weight ~13.4 grams or 12.7 mm PTFE balls ~2.3 grams); (2) PTFE milling jars (15 mm SS balls ~13.4 grams or 12.7 mm PTFE balls ~2.3 grams); § and (3) Al milling jars (12.7 mm PTFE balls ~2.3 grams). Then, NMR of the crude product was taken for yield determination and the remaining product was purified and analysed by PXRD.

3. Results and discussion

The synthesis of tolbutamide has been reported to readily provide 60–80% yields upon milling with different copper salts without any atmosphere control.[37,38] Surprisingly, our attempts to conduct the reaction under a dry N_2 atmosphere gave conversions of 0–5% by either neat milling or LAG. Deliberate addition of 1–30 μL water into the reaction mixture did not improve conversion, indicating that using an air-free environment, regardless of the presence of moisture, was deleterious for the reaction. Indeed, running the reaction under dried air led to improved conversions (~80% for LAG, ~50% for neat milling).

These observations suggested that oxygen plays a critical role for this copper-catalysed coupling. This was further validated by developing a system for the precise mixing of dried air and N_2 gases, enabling a systematic study of the effect of atmospheric oxygen content on tolbutamide formation. Recording reaction conversion at gas phase O_2 amounts of 0.00 (*i.e.*, pure N_2), 0.057, 0.10, 0.14, and 0.22 mmol (calculated assuming ideal gas conditions from measured O_2 percentages of 0.0, 5.5, 10.0, 13.7, and 20.9% respectively) revealed a clear dependence of tolbutamide formation on oxygen amount (see Fig. 2). For each oxygen level, conversion was calculated as an average of four separate measurements.

Conversion was found to increase with oxygen content. This trend was more reliable for reactions using LAG, while for neat milling, the variation in yield was much more significant across the repeated measurements for each oxygen concentration. The high variability of the conversion in neat milling reactions,

‡ Throughout the manuscript stainless steel is abbreviated as SS, polytetrafluoroethylene as PTFE, and bulk aluminium metal as Al.

§ Previous reports on LAG synthesis of tolbutamide used 10 mL volume SS jars with a single SS ball of 10 mm diameter and reported polymorph 1 and polymorph 2 formation.[37,38]

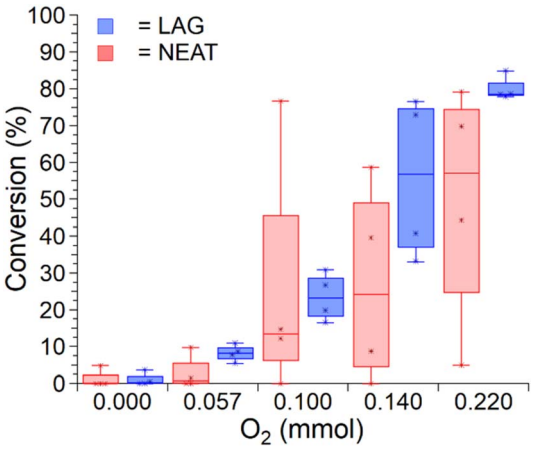

Fig. 2 Conversion of the copper-catalysed sulfonamide-isocyanate coupling to form tolbutamide as a function of atmospheric oxygen content measured is shown as a box and whiskers plot. Each data point is the average of four repeated experiments shown as starred points at the respective yields observed. Bars show lowest and highest yield observed at each oxygen concentration (see Section 3.2 of the ESI† for more details). See Section 3.1 of the ESI† for an important cautionary note regarding yield determination by NMR.

compared to LAG, suggests that the presence of a liquid additive enables more efficient mixing of the sample with a gas. Such a result is consistent with previous reports that adding a small amount of a liquid to a mechanochemical mixture enables greater powder flowability, promoting mixing.[51]

The observed effect of oxygen on tolbutamide formation was not previously reported and suggests either the need for pre-oxidation or disproportionation of the CuCl catalytic additive into Cu(II) or that the coupling reaction is inherently based on a redox process. In order to distinguish between these two possibilities, the reaction was repeated in the presence of dry brown anhydrous $CuCl_2$ (5 mol%) as the catalyst (see Section 2.7). In contrast to previous trials with CuCl, reaction under dry N_2 atmosphere now led to 73% conversion by LAG, and 75% by neat milling within 2 hours.

These observations suggest that the catalytic species in tolbutamide synthesis is Cu(II) based, and that the role of atmospheric oxygen in CuCl-based reactions is to convert CuCl to catalytically active Cu(II). Thus, as the oxygen amount increases relative to the amount of Cu(I), the yield of the reaction increases. Given we were using 0.0625 mmol CuCl, we tested the reaction with mol ratios of O_2 to Cu(I) of 0 : 1, 0.9 : 1, 1.6 : 1, 2.2 : 1, and 3.5 : 1 corresponding to 0, 0.057, 0.1, 0.14, and 0.22 mmol O_2 (see Fig. 2). Thus, sufficient conversion of copper to the active form for restored reactivity occurs when 3.5 equivalents of oxygen is added roughly corresponding to the amount available in dry air.

The claim for Cu(II) as the active catalyst is further supported by X-ray photoelectron spectroscopy (see Fig. 3a and b) of the crude reaction mixture for the initially CuCl-containing LAG process, performed under either dry air or N_2. Analysis by XPS (see Fig. 3a and b) reveals that Cu(I) is in excess when the reaction is run under nitrogen, while Cu(II) is in excess when the reaction is run in dry air (see also Section 7 of the ESI†). Overall, these observations strongly indicate Cu(II) as the catalytic species, with commonly used CuCl actually acting as a pre-catalyst. It is worth noting that Cu metal likely undergoes a similar oxidation process when driving the reaction mechanocatalytically as in previous reports with brass.[37]

Current studies exploring the surface chemistry of the copper and the phenomenon of mechanocatalysis with this established methodology are underway in our labs using Cu milling balls.

Next, we evaluated the potential effect of the milling assembly material on the reaction, by milling with different combinations of steel, PTFE, and Al jars with SS or PTFE balls. After milling in dry air (see Table 1 and Section 2.1 of the ESI†) the reaction conversions were generally higher with $CuCl_2$ as the catalytic additive, consistent with the observation that CuCl requires prior oxidation to Cu(II). This is particularly evident in the slower neat milling reactions, where conversions generally

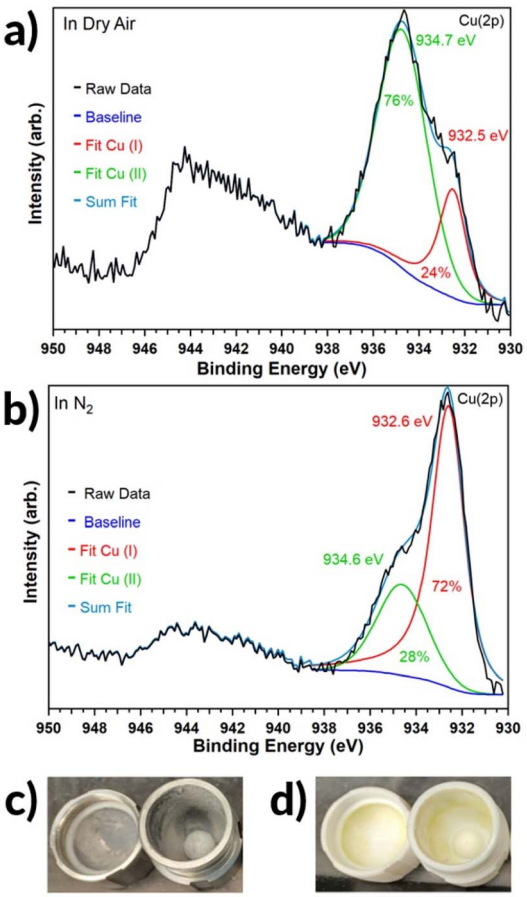

Fig. 3 X-ray photoelectron spectra of the Cu $2p_{3/2}$ signal with fit for Cu(I) and Cu(II) regions for samples milled in: (a) dry air and (b) dry nitrogen. It was not possible to distinguish between CuCl and other potentially formed other copper(I) species, such as Cu_2O, due to similar binding energies in the Cu $2p_{3/2}$ region. $CuCl_2$ is distinct in binding energy from CuO and is clearly identified. Photographs of the reactions performed by milling with CuCl in dry air using: (c) Al and (d) PTFE jars. Note: the broad feature between 938–946 eV is a shake-up feature associated with Cu(II).

lie in the range of 40–50% with CuCl (exempting the reaction in PTFE jar with a SS ball), and in the 75–85% range with $CuCl_2$.

A striking result of screening different milling assembly materials under dry air conditions is the complete loss of reactivity (with CuCl as the catalyst), when using the Al-based jars with PTFE balls (see Table 1). Here, 0% conversions were obtained whether milling neat, or under LAG conditions, or in air that was not dried (45% relative humidity). The loss of reactivity is not due to the use of PTFE balls, as switching to SS or PTFE jars readily gave tolbutamide even with PTFE balls. Tentatively, we explain the deactivation of the reaction by the jar Al metal hindering the oxidation of CuCl. This is supported by the appearance of reaction mixtures containing CuCl, which, when Al jars were used, remained white (see Fig. 3c, also Section 6 of the ESI†). This is supported by the appearance of reaction mixtures containing CuCl, which, when Al jars were used, remained white (see Fig. 3c, also Section 6 of the ESI†). In contrast, the corresponding reaction mixtures in all other cases turned yellow-green, consistent with oxidation of CuCl (see Fig. 3d, also Section 6 of the ESI†). Furthermore, reaction with $CuCl_2$ in Al jars provided 72% conversion by LAG and 76% conversion by neat milling. Identification of Cu(II) as the catalytic species provides the first solid, although preliminary, hints towards a mechanism for this reaction. It seems likely that Cu(II) could facilitate the reaction by coordination to the sulfonamide reactant and, potentially, N–H bond insertion.

We hypothesize three potential mechanisms for aluminium mechanoinhibition. The first possibility is that aluminium metal acts as an oxygen scavenger forming Al_2O_3 *in situ* when the native oxide is stripped from the metal surface by the milling process ($Al(0) + O_2 \rightarrow Al_2O_3$, $\Delta G = -1582$ kJ mol^{-1}), thus preventing the Cu(I) from reacting with available oxygen to oxidize to Cu(II).[52] The observation of a greyish tinge to the mixture suggesting aluminium wear in the product and the large Gibbs free energy for this transformation supports this theory. Amorphous aluminium oxide formed in the milling process could also be acting to stabilize the Cu(I) state; thus disfavouring oxidization to Cu(II) as shown recently by Jia *et al.*[53] An alternative theory would be the reduction of oxidized copper by aluminium directly ($\Delta G = -636$ kJ mol^{-1} for Al(0) + Cu(I) → Al(III) + Cu(0) and $\Delta G = -1168$ kJ mol^{-1} for Al(0) + Cu(II) → Al(III) + Cu(0)).[54,55] On this theory, stainless steel does not show a corresponding mechanoinhibition effect due to the small Gibbs free energy for Cu reduction with Fe ($\Delta G = -151$ kJ mol^{-1} for Fe(0) + Cu(II) → Fe(II) + Cu(0) and $\Delta G = -15$ kJ mol^{-1} for Fe(0) + Cu(I) → Fe(II) + Cu(0)).[54,55] Investigations to elucidate which phenomenon are occurring are currently underway.

To further explore the effect of catalyst choice, a variety of metal(II) chlorides were examined under controlled dry air atmosphere (see Table 2). Reactions were run with 5 mol% of potential catalyst in SS jars with SS balls according to the established procedure. Product yield with all these explored alternative metal chlorides was found to be poor, which is in accordance with previous reports, never exceeding 10%.[37,38]

In the interest of promoting atom economy,[5,56] the effect of $CuCl_2$ catalyst loading and reaction time on product yield was examined. Using $CuCl_2$ as the catalytic additive permitted reaction yields ranging from 60–85% within 30 minutes. For exploration of the effect of catalyst loading, however, we decided to maintain a 2 hours reaction time as the observed yield is less reproducible trial to trial with shorter reaction time. By employing Cu(II) directly, catalyst loading was readily reduced from 5 mol% to 1 mol% (see Fig. 4 and Section 10 of the ESI†), which is significantly lower than in previous reports. Moreover, at similar reaction times, low yields were observed using $CuCl_2$ in DMSO-d_6 solution at room temperature; revealing the mechanochemical reaction is more efficient (see Section 3.1 of ESI†). An interesting note was the increase in conversion by ~10% upon reducing the loading of the catalytic additive (see Fig. 4). We suspect excess $CuCl_2$ plays a similar role to a bulk inert additive, and hampers diffusion of reactants generally slowing product formation. Investigations along these lines are underway.

As a final feature of interest, it is worth noting that while LAG generally leads to better reaction repeatability when employing

Table 1 Conversion to tolbutamide (in %) upon LAG or neat milling in dry air using jars and balls made from different materials, using CuCl or $CuCl_2$ as the catalytic additive[a]

			Conversion (%)	
Additive	Jar	Ball[b]	LAG	Neat milling
CuCl	SS	SS	80	50
CuCl	SS	PTFE	82	43
CuCl	PTFE	SS	78	90
CuCl	PTFE	PTFE	64	40
CuCl	Al	PTFE	0[c]	0[c]
$CuCl_2$	SS	SS	73	75
$CuCl_2$	SS	PTFE	79	85
$CuCl_2$	PTFE	SS	65	80
$CuCl_2$	PTFE	PTFE	77	82
$CuCl_2$	Al	PTFE	72	76

[a] LAG reactions were conducted in presence of nitromethane ($\eta = 0.25$ μL mg^{-1}) as the liquid additive. [b] SS balls of 15 mm diameter (weight ~13.4 grams) were used, while PTFE balls had a diameter of 12.7 mm (weight ~2.3 grams). [c] 0% conversion was also observed when the reactions were conducted in atmospheres that were not dried. See Section 3.1 of the ESI for an important cautionary note regarding yield determination by NMR.

Table 2 Conversion to tolbutamide (in %) upon LAG or neat milling in SS jars with SS balls under dry air using a metal (II) chloride as the catalytic additive[a]

	Conversion (%)	
Catalyst	LAG	Neat milling
$CaCl_2 \cdot 2H_2O$	0.0	0.0
$MnCl_2 \cdot 4H_2O$	0.0	0.0
$CoCl_2$	3.3	0.0
$NiCl_2$	2.5	2.8
$CuCl_2$	71	76
$ZnCl_2$	8.2	6.0
$CdCl_2 \cdot H_2O$	0.0	0.0

[a] LAG reactions were conducted in presence of nitromethane ($\eta = 0.25$ μL mg^{-1}) as the liquid additive.

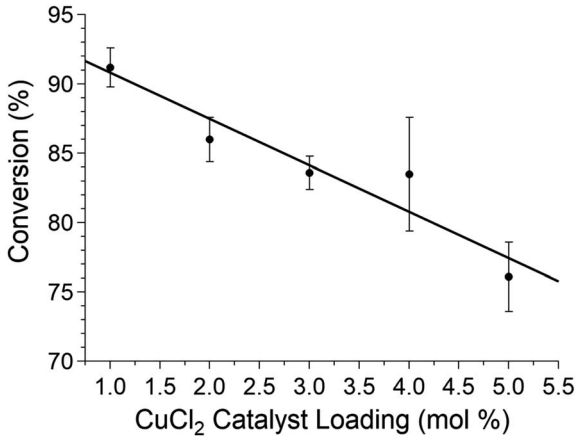

Fig. 4 Conversion of the copper-catalysed sulfonamide-isocyanate coupling to form tolbutamide under dry air in SS jars with SS balls as a function of catalyst loading in neat grinding conditions (see Section 10 of the ESI† for similar trials with LAG). Each data point is the average of three repeated experiments and error is shown as standard deviation. Lines are intended to guide the eye. See Section 3.1 of the ESI† for a cautionary note regarding yield determination by NMR.

the traditional CuCl catalyst (see Fig. 2), this phenomenon does not translate to the true $CuCl_2$ catalyst system. When employing $CuCl_2$ in LAG conditions (see Fig. 3, 4, and Section 10 of the ESI†), conversions are statistically identical to the reaction when performed in neat conditions with similar standard deviations to neat trials. This aligns with previous results showing similar conversions between neat $CuCl_2$ and LAG CuCl.[37] These findings suggest that, while LAG generally increases conversion mechanochemically, it is not beneficial in this reaction system. Thus, atom economy can likely be increased by avoiding LAG reagents for these transformations in future.

4. Conclusions

In summary, we have provided a systematic overview of parameters related to the milling assembly and atmosphere, which permitted the identification of Cu(II) as the most likely catalytic species in the mechanochemical model reaction of tolbutamide synthesis. This outcome indicates that typically used CuCl likely plays the role of a pre-catalyst, which becomes activated through aerobic oxidation. By employing $CuCl_2$, catalyst loading can be reduced significantly. Moreover, screening of different materials for milling jars and balls also revealed what appears to be the first example of a catalytic mechanochemical reaction being shut down by the choice of a particular milling jar material. Specifically, milling in an Al jar led to complete inhibition of the coupling reaction, in the presence of either dry or humid air, which is tentatively attributed to preventing aerobic oxidation of CuCl pre-catalyst. We term such behavior direct mechanoinhibition, highlighting it as the opposite of the now well-established direct mechanocatalysis phenomenon. Direct mechanoinhibition demonstrates the ability to tune mechanochemical milling surfaces not only to promote reactivity[34–36,57] but also to switch off reactions. It was also shown that excess catalyst in a mechanochemical reaction can reduce reaction efficiency; a phenomenon we are actively exploring. These results illustrate how focusing on mechanochemical reaction parameters other than catalyst and/or additive choice can lead to important conclusions even in well-established reaction systems, and we hope they will encourage further systematic studies of mechanocatalysis.

Author contributions

Author contributions to this work according to CRediT standardised contribution descriptions are as follows: Kathleen Floyd (conceptualization, data curation, formal analysis, investigation, methodology, visualization, validation, writing-original draft, writing-review and editing), Lori Gonett (conceptualization, formal analysis, methodology, writing-review & editing), Tomislav Friščić (conceptualization, project administration, formal analysis, supervision, writing-review & editing), and James Batteas (conceptualization, funding acquisition, project administration, resources, supervision, writing-review & editing).

Conflicts of interest

There are no conflicts to declare.

Acknowledgements

We thank F. Mangolini, H.-M. Lien, and Dr Jing Wu for assistance in XPS, Dr N. Bhuvanesh for help with PXRD, Dr Gregory Wylie and Dr Doug Elliot for assistance in NMR, and Dr Y. Rezenom for LC-MS ESI analyses. We also thank the Youth Adventure Program: Smash Chemistry at Texas A&M and students: John Bless, Cody Chang, Alexis Grammar, Madelyn Gray, and Jacob Hinojosa, whose studies provided the initial inspiration for this project. The work was supported by the NSF Center for the Mechanical Control of Chemistry under grants CHE-2023644 and CHE-2303044. We thank the Leverhulme Trust for Leverhulme International Professorship (TF) and University of Birmingham.

Notes and references

1 S. L. James, C. J. Adams, C. Bolm, D. Braga, P. Collier, T. Friščić, F. Grepioni, K. D. M. Harris, G. Hyett, W. Jones, A. Krebs, J. Mack, L. Maini, A. G. Orpen, I. P. Parkin, W. C. Shearouse, J. W. Steed and D. C. Waddell, *Chem. Soc. Rev.*, 2012, **41**, 413–447.
2 A. A. L. Michalchuk, E. V. Boldyreva, A. M. Belenguer, F. Emmerling and V. V. Boldyrev, *Front. Chem.*, 2021, **9**, e2021.685789.
3 T. Friščić, C. Mottillo and H. M. Titi, *Angew. Chem., Int. Ed.*, 2020, **59**, 1018–1029.
4 V. Martinez, T. Stolar, B. Karadeniz, I. Brekalo and K. Užarević, *Nat. Rev. Chem*, 2023, **7**, 51–65.
5 K. J. Ardila-Fierro and J. G. Hernández, *ChemSusChem*, 2021, **14**, 2145–2162.

6 O. Galant, G. Cerfeda, A. S. McCalmont, S. L. James, A. Porcheddu, F. Delogu, D. E. Crawford, E. Colacino and S. Spatari, *ACS Sustain. Chem. Eng.*, 2022, **10**, 1430–1439.
7 F. Schneider, T. Szuppa, A. Stolle, B. Ondruschka and H. Hopf, *Green Chem.*, 2009, **11**, 1894–1899.
8 R. B. N. Baig and R. S. Varma, *Chem. Soc. Rev.*, 2012, **41**, 1559–1584.
9 T. Friščić, S. L. Childs, S. A. A. Rizvi and W. Jones, *CrystEngComm*, 2009, **11**, 418–426.
10 T. Friščić, *Chem. Soc. Rev.*, 2012, **41**, 3493–3510.
11 J. G. Hernández and C. Bolm, *J. Org. Chem.*, 2017, **82**, 4007–4019.
12 F. Cuccu, L. De Luca, F. Delogu, E. Colacino, N. Solin, R. Mocci and A. Porcheddu, *ChemSusChem*, 2022, **15**, e202200362.
13 P. A. Julien, C. Mottillo and T. Friščić, *Green Chem.*, 2017, **19**, 2729–2747.
14 T. Stolar and K. Užarević, *CrystEngComm*, 2020, **22**, 4511–4525.
15 B. P. Biswal, S. Chandra, S. Kandambeth, B. Lukose, T. Heine and R. Banerjee, *J. Am. Chem. Soc.*, 2013, **135**, 5328–5331.
16 S. T. Emmerling, L. S. Germann, P. A. Julien, I. Moudrakovski, M. Etter, T. Friščić, R. E. Dinnebier and B. V. Lotsch, *Chem*, 2021, **7**, 1639–1652.
17 N. Davison, J. A. Quirk, F. Tuna, D. Collison, C. L. McMullin, H. Michaels, G. H. Morritt, P. G. Waddell, J. A. Gould, M. Freitag, J. A. Dawson and E. Lu, *Chem*, 2023, **9**, 576–591.
18 P. Ying, J. Yu and W. Su, *Adv. Synth. Catal.*, 2021, **363**, 1246–1271.
19 D. Tan, L. Loots and T. Friščić, *Chem. Commun.*, 2016, **52**, 7760–7781.
20 A. Porcheddu, F. Delogu, L. De Luca, C. Fattuoni and E. Colacino, *Beilstein J. Org. Chem.*, 2019, **15**, 1786–1794.
21 A. Porcheddu, E. Colacino, L. De Luca and F. Delogu, *ACS Catal.*, 2020, **10**, 8344–8394.
22 P. Shi, Y. Tu, D. Zhang, C. Wang, K.-N. Truong, K. Rissanen and C. Bolm, *Adv. Synth. Catal.*, 2021, **363**, 2552–2556.
23 J.-H. Schöbel, P. Elbers, K.-N. Truong, K. Rissanen and C. Bolm, *Adv. Synth. Catal.*, 2021, **363**, 1322–1329.
24 K. Kubota, T. Seo, K. Koide, Y. Hasegawa and H. Ito, *Nat. Commun.*, 2019, **10**, 111.
25 T. Seo, K. Kubota and H. Ito, *J. Am. Chem. Soc.*, 2023, **145**, 6823–6837.
26 R. R. A. Bolt, S. E. Raby-Buck, K. Ingram, J. A. Leitch and D. L. Browne, *Angew. Chem., Int. Ed.*, 2022, **61**, e202210508.
27 M. Carta, A. L. Sanna, A. Porcheddu, S. Garroni and F. Delogu, *Sci. Rep.*, 2023, **13**, 2470.
28 D. Kong and C. Bolm, *Green Chem.*, 2022, **24**, 6476–6480.
29 R. Thorwirth, A. Stolle and B. Ondruschka, *Green Chem.*, 2010, **12**, 985–991.
30 T. Szuppa, A. Stolle, B. Ondruschka and W. Hopfe, *Green Chem.*, 2010, **12**, 1288–1294.
31 D. Braga, S. L. Giaffreda, F. Grepioni and M. Polito, *CrystEngComm*, 2004, **6**, 459–462.
32 M. J. Rak, N. K. Saadé, T. Friščić and A. Moores, *Green Chem.*, 2014, **16**, 86–89.
33 G. Štefanić, S. Krehula and I. Štefanić, *Chem. Commun.*, 2013, **49**, 9245–9247.
34 C. G. Vogt, S. Grätz, S. Lukin, I. Halasz, M. Etter, J. D. Evans and L. Borchardt, *Angew. Chem., Int. Ed.*, 2019, **58**, 18942–18947.
35 R. A. Haley, A. R. Zellner, J. A. Krause, H. Guan and J. Mack, *ACS Sustain. Chem. Eng.*, 2016, **4**, 2464–2469.
36 L. Chen, D. Leslie, M. G. Coleman and J. Mack, *Chem. Sci.*, 2018, **9**, 4650–4661.
37 D. Tan, V. Štrukil, C. Mottillo and T. Friščić, *Chem. Commun.*, 2014, **50**, 5248–5250.
38 E. Colacino, G. Dayaker, A. Morère and T. Friščić, *J. Chem. Educ.*, 2019, **96**, 766–771.
39 D. Tan, C. Mottillo, A. D. Katsenis, V. Štrukil and T. Friščić, *Angew. Chem., Int. Ed.*, 2014, **53**, 9321–9324.
40 G. Dayaker, D. Tan, N. Biggins, A. Shelam, J.-L. Do, A. D. Katsenis and T. Friščić, *ChemSusChem*, 2020, **13**, 2966–2972.
41 L. Gonnet, C. B. Lennox, J.-L. Do, I. Malvestiti, S. G. Koenig, K. Nagapudi and T. Friščić, *Angew. Chem., Int. Ed.*, 2022, **61**, e202115030.
42 S. Reichle, M. Felderhoff and F. Schüth, *Angew. Chem., Int. Ed.*, 2021, **60**, 26385–26389.
43 F. Puccetti, T. Rinesch, S. Suljić, K. Rahimi, A. Herrmann and C. Bolm, *Chem*, 2023, **9**, 1318–1332.
44 J. Cervelló and T. Sastre, *Synthesis*, 1990, 221–222.
45 C. G. Vogt, M. Oltermann, W. Pickhardt, S. Grätz and L. Borchardt, *Adv. Energy Sustainability Res.*, 2021, **2**, 2100011.
46 S. Hwang, S. Grätz and L. Borchardt, *Chem. Commun.*, 2022, **58**, 1661–1671.
47 W. Pickhardt, S. Grätz and L. Borchardt, *Chem. –A Euro. J.*, 2020, **26**, 12903–12911.
48 M. Wohlgemuth, M. Mayer, M. Rappen, F. Schmidt, R. Saure, S. Grätz and L. Borchardt, *Angew. Chem., Int. Ed.*, 2022, **61**, e202212694.
49 C. B. Lennox, T. H. Borchers, L. Gonnet, C. J. Barrett, S. G. Koenig, K. Nagapudi and T. Friščić, *Chem. Sci.*, 2023, **14**, 7475–7481.
50 S. Thirunahari, S. Aitipamula, P. S. Chow and R. B. H. Tan, *J. Pharm. Sci.*, 2010, **99**, 2975–2990.
51 O. V. Lapshin, E. V. Boldyreva and V. V. Boldyrev, *Russ. J. Inorg. Chem.*, 2021, **66**, 433–453.
52 *NIST Standard Reference Database Number 69*, ed. P. J. L. W. G. Mallard, National Institute of Standards and Technology, Gaithersburg MD, 20899, 2023.
53 H. Cheng, S. Jia, J. Jiao, X. Chen, T. Deng, C. Xue, M. Dong, J. Zeng, C. Chen, H. Wu, M. He and B. Han, *Green Chem.*, 2024, **26**, 2599–2604.
54 A. J. Bard, *Standard Potentials in Aqueous Solution*, 1st edn, Routledge, 1985.
55 G. Milazzo, S. Caroli and V. K. Sharma, *Tables of standard electrode potentials / by Guilio Milazzo and Sergio Caroli, with the cooperation of V. K. Sharma*, Wiley, New York, 1977.
56 P. Anastas and N. Eghbali, *Chem. Soc. Rev.*, 2010, **39**, 301–312.
57 T. L. Cook, J. A. Walker and J. Mack, *Green Chem.*, 2013, **15**, 617–619.